

Improvement of critical current density in MgB₂ superconductors by Zr doping at ambient pressure

Author:

Feng, Y; Zhao, Yong; Sun, Y; Liu, F.C.; Fu, B.Q.; Zhou, L.; Cheng, C.H.; Koshizuka, N; Murakami, M

Publication details:

Applied Physics Letters

v. 79

Chapter No. 24

pp. 3983-3985

0003-6951 (ISSN)

Publication Date:

2001

Publisher DOI:

<http://dx.doi.org/10.1063/1.1426264>

License:

<https://creativecommons.org/licenses/by-nc-nd/3.0/au/>

Link to license to see what you are allowed to do with this resource.

Downloaded from <http://hdl.handle.net/1959.4/39075> in <https://unsworks.unsw.edu.au> on 2024-04-19

Improvement of critical current density in MgB_2 superconductors by Zr doping at ambient pressure

Y. Feng^{a)}

*Superconductivity Research Laboratory, ISTE, 10-13 Shinonome, 1-chome, Koto-ku, Tokyo 135, Japan
and Northwest Institute for Nonferrous Metal Research, P.O. Box 51, Xi'an, Shaanxi 710016,
People's Republic of China*

Y. Zhao

*Superconductivity Research Laboratory, ISTE, 10-13 Shinonome, 1-chome, Koto-ku, Tokyo 135, Japan and
School of Materials Sciences and Engineering, University of New South Wales, Sydney, 2052, NSW
Australia*

Y. P. Sun, F. C. Liu, B. Q. Fu, L. Zhou, and C. H. Cheng

*Northwest Institute for Nonferrous Metal Research, P.O. Box 51, Xi'an, Shaanxi 710016,
People's Republic of China*

N. Koshizuka, and M. Murakami

Superconductivity Research Laboratory, ISTE, 10-13 Shinonome, 1-chome, Koto-ku, Tokyo 135, Japan

(Received 12 September 2001; accepted for publication 17 October 2001)

We present the superconducting properties and phase compositions of $\text{Mg}_{1-x}\text{Zr}_x\text{B}_2$ bulk samples fabricated by a solid-state reaction at ambient pressure. It is found that a small amount of Zr atoms may be introduced into the lattice of MgB_2 , while the majority of them forms ZrB_2 phase. The $\text{Mg}_{0.9}\text{Zr}_{0.1}\text{B}_2$ sample shows the highest J_C of $2.1 \times 10^6 \text{ A/cm}^2$ in 0.56 T at 5 K and $1.83 \times 10^6 \text{ A/cm}^2$ in self-field at 20 K, higher irreversibility field and larger upper critical field in MgB_2 bulk samples. The combination of good grain connection, the reduction of grain size and small ZrB_2 particles in the sample may be responsible for the significant enhancement of J_C in Zr-doped samples. This technique has a great potential to prepare high performance MgB_2 bulk samples and wires on an industrial scale. © 2001 American Institute of Physics.
[DOI: 10.1063/1.1426264]

The recent discovery of superconductivity at 39 K in binary intermetallic compound MgB_2 has attracted much more interest.¹ The critical temperature T_C value of MgB_2 is much higher than the previous record T_C of 23 K for the A15 compound Nb_3Ge . Unlike high- T_C superconductors, MgB_2 has no weak link at the grain boundaries.² It is found that MgB_2 is a typical type-II superconductor, very similar to Nb_3Sn except for the extremely high T_C .^{3,4} Unfortunately, the MgB_2 bulk samples prepared under ambient pressure have a low J_C (the highest J_C is around $2 \times 10^5 \text{ A/cm}^2$ at 10 K in zero field) due to the bad connection between grains and poor flux pinning.⁵ To date, high quality MgB_2 bulk samples have been fabricated by using high pressure.^{6,7} The typical J_C value of these samples could reach $2 \times 10^4 \text{ A/cm}^2$ at 20 K in 1 T.⁶ It is also reported that dense MgB_2 bulks with J_C of $1.4 \times 10^6 \text{ A/cm}^2$ at zero temperature can be obtained by using hot isostatic pressing.⁸ Although these techniques, including high pressure sintering and proton irradiation, can be used to improve the flux pinning,⁹ they suffer from the technical problems and are not suitable for the fabrication of MgB_2 wires and tapes. On the other hand, the chemical doping is found to be easily controlled, nondestructive and highly efficient in improving microstructure and flux pinning in high- T_C superconductors.¹⁰ Very recently, it was observed that the partial substitution of Zn or Cu for Mg in MgB_2 led to a

reduction of T_C .¹¹ In addition, contrary to an article describing a deleterious effect of Ti doping,¹² a previous study shows a suitable amount of Ti doping will increase J_C in MgB_2 .¹³

In this letter, magnetization, x-ray diffraction results and microstructure features in Zr-doped MgB_2 bulk samples are reported. The results indicate that the Zr doping can significantly enhance the flux pinning. The J_C value of $2.1 \times 10^6 \text{ A/cm}^2$ in 0.56 T at 5 K has been obtained in $\text{Mg}_{0.9}\text{Zr}_{0.1}\text{B}_2$, which is much higher than the best result reported so far in MgB_2 bulks.

The samples with nominal compositions of $\text{Mg}_{1-x}\text{Zr}_x\text{B}_2$ ($x=0, 0.05, 0.1$, and 0.2) were fabricated by the solid-state reaction method at ambient pressure by using the high purity powders of Mg (99%), Zr (99%), and B (99%). The precursor powders were fully mixed and were cold pressed into small cylindrical pellets. Then, the pellets were put on a Ta plate and heat treated at the temperature region of 600 °C to 900 °C for 3 h in flowing argon without high pressure. Finally, the pellets were followed by a furnace cooling to room temperature. Magnetization was measured by a superconducting quantum interference device magnetometer (Quantum Design, MPMSR2) at different temperatures in the magnetic field up to 7 T. J_C values were deduced from the magnetization curves using the Bean critical model.¹⁴ The phase composition analysis of all samples was carried out by an ac 10000 x-ray diffractometer with a Cu $K\alpha$ irradiation.

^{a)}Author to whom correspondence should be addressed; electronic mail: yfeng@c-nin.com

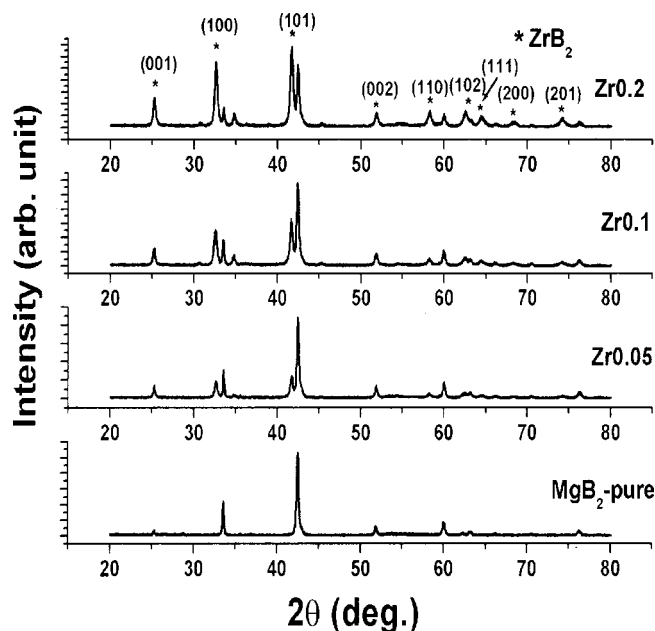


FIG. 1. X-ray diffraction patterns for all samples. ZrB_2 phase is found in Zr-doped specimens.

All the samples for this study have the same dimensions of $0.7 \times 0.9 \times 1.4 \text{ mm}^3$.

X-ray diffraction patterns for all samples are shown in Fig. 1. The results show that the MgB_2 crystalline grains in the sample are not textured. It can be observed that the ZrB_2 phase is formed besides the MgB_2 phase and the amount of ZrB_2 increases with an increase of Zr content in Zr-doped samples. The molar percentage of ZrB_2 in the samples increases from 3.63% in $\text{Mg}_{0.95}\text{Zr}_{0.05}\text{B}_2$ to 14% in $\text{Mg}_{0.8}\text{Zr}_{0.2}\text{B}_2$. Furthermore, the lattice parameters are calculated by the least-square fitting. The a axis increases with an increase of the doping level and the c axis remains almost unchanged, which indicates that a small amount of Zr atoms may be a substitute for Mg in the lattice of MgB_2 . However, the lattice constants in the sample with $x=0.2$ are the same as those in $\text{Mg}_{0.9}\text{Zr}_{0.1}\text{B}_2$, implying that the solubility limit is achieved in the sample with $x=0.1$.

Figure 2 shows the temperature dependence of magnetization for all the samples at 20 Oe. It can be seen that critical

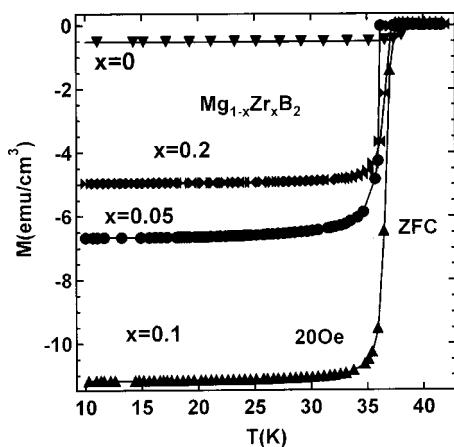


FIG. 2. Temperature dependent magnetization curves measured in ZFC condition at 20 Oe for all samples. The sample with $x=0.1$ has the maximum diamagnetic signal.

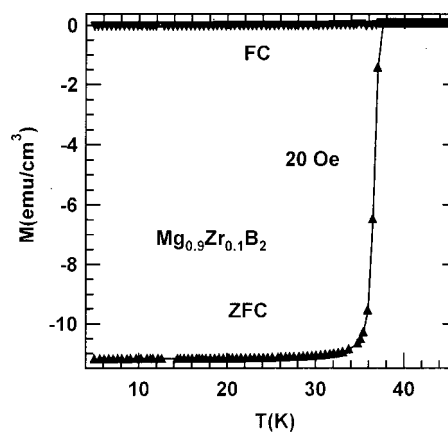


FIG. 3. Temperature dependence of magnetization in ZFC and FC conditions for $\text{Mg}_{0.9}\text{Zr}_{0.1}\text{B}_2$ at 20 Oe.

temperature changes with Zr doping and slightly decreases from 38.4 K in pure MgB_2 to 37.3 K in $\text{Mg}_{0.8}\text{Zr}_{0.2}\text{B}_2$. The slight variation of the T_C in Zr-doped samples may be due to the partial substitution of Zr for Mg. The expansion of the a axis results in the reduction of T_C in Zr-doped specimens, which gives evidence of the model of hole superconductivity in MgB_2 .¹⁵ In this model, it is predicted that the increase of the a axis will decrease the T_C . It is noted that the sample with $x=0.1$ displays a superconducting transition at 37.3 K with a sharp transition width of 0.7 K, suggesting the phase homogeneity and good connection between grains. In addition, $\text{Mg}_{0.8}\text{Zr}_{0.2}\text{B}_2$ has the same T_C as the sample with $x=0.1$, but the transition width becomes slightly larger. This may be attributed to the solubility limit and more second phases existing in the sample. As shown in Fig. 3, the transitions in zero-field cooling (ZFC) and field-cooling (FC) processes for $\text{Mg}_{0.9}\text{Zr}_{0.1}\text{B}_2$ are dramatically separated, confirming the strong flux trapping in the sample with $x=0.1$.

Figure 4 illustrates the J_C value as a function of magnetic field at selected temperatures for the samples with $x=0, 0.05$ and 0.1 . All the Zr-doped samples have a higher J_C than pure MgB_2 . Within all temperatures and the whole field region up to 7 T, the J_C value of the sample with $x=0.1$ is the highest amount these samples. It can be seen from Fig. 4 that J_C achieves $2.1 \times 10^6 \text{ A/cm}^2$ in 0.56 T and

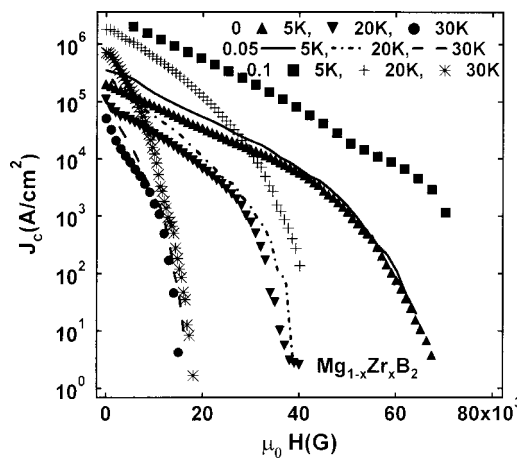


FIG. 4. J_C versus magnetic field at 5, 20, and 30 K for the samples with $x=0, 0.05$ and 0.1 . Note that J_C in $\text{Mg}_{0.9}\text{Zr}_{0.1}\text{B}_2$ is very high about $2.1 \times 10^6 \text{ A/cm}^2$ in 0.56 T at 5 K.

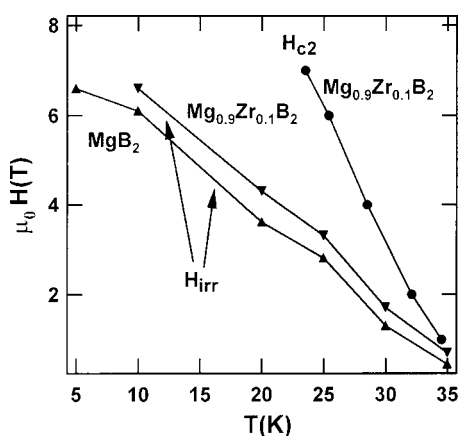


FIG. 5. Irreversibility fields as a function of temperature for pure MgB_2 and $\text{Mg}_{0.9}\text{Zr}_{0.1}\text{B}_2$ samples. The H_{c2} data for the sample with $x=0.1$ is also shown.

$5.7 \times 10^5 \text{ A/cm}^2$ in 2 T at 5 K for the $\text{Mg}_{0.9}\text{Zr}_{0.1}\text{B}_2$ sample. At 20 K, J_C is as high as $1.83 \times 10^6 \text{ A/cm}^2$ in self-field, $5.51 \times 10^5 \text{ A/cm}^2$ in 1 T and $1.22 \times 10^5 \text{ A/cm}^2$ in 2 T. Also, J_C reaches $7.2 \times 10^5 \text{ A/cm}^2$ in self-field and $1.2 \times 10^4 \text{ A/cm}^2$ in 1 T even at 30 K. These J_C values are much higher than the best data on the MgB_2 bulk samples including proton-irradiated fragments, hot isostatic pressed sample and MgB_2 specimen prepared under high pressure. The Zr doping in MgB_2 opens up an effective and easily controlled method to improve J_C . It should be noted that this technique is very suitable for the industrial scale fabrication of MgB_2 bulks and wires because the Zr-doped samples are prepared at ambient pressure.

Moreover, the temperature dependence of the irreversibility fields H_{irr} for pure MgB_2 and $\text{Mg}_{0.9}\text{Zr}_{0.1}\text{B}_2$ samples is shown in Fig. 5. The Zr doping also results in an improvement of H_{irr} . At 20 K, H_{irr} is increased from 3.6 T in pure MgB_2 to 4.3 T in $\text{Mg}_{0.9}\text{Zr}_{0.1}\text{B}_2$. The irreversibility field in the sample with $x=0.1$ is much higher than those in the dense MgB_2 samples due to high pressure sintering. In addition, the upper critical field H_{c2} for $\text{Mg}_{0.9}\text{Zr}_{0.1}\text{B}_2$ is also given in Fig. 5. The slope of the $H_{c2}-T$ curve is $dH_{c2}/dT = -0.56 \text{ T/K}$, which yields a higher upper critical field $H_{c2}(0) = 20 \text{ T}$ in MgB_2 bulks.

The mechanism for the significant enhancement of critical current density may be related to the very strong pinning force and its high density in Zr-doped MgB_2 . First, the connection between the grains is much improved in Zr-doped samples. As the doping content increases, the density and J_C value increase. The density of the Zr-doped sample is even higher than that of the MgB_2 specimens prepared under high pressure. However, the best microstructure is achieved in $\text{Mg}_{0.9}\text{Zr}_{0.1}\text{B}_2$. Secondly, the grain boundary pinning is very strong in MgB_2 like Nb_3Sn . The flux pinning force density is found to be inversely proportional to the grain size in Nb_3Sn .¹⁶ The grain size of MgB_2 is reduced in the samples with high doping level. The average grain size in $\text{Mg}_{0.95}\text{Zr}_{0.05}\text{B}_2$ is around 90 nm, almost the same as that in pure MgB_2 . When Zr content is increased to $x=0.1$, the average grain size is decreased to 60 nm, which will greatly

enhance the flux pinning. The grain size in $\text{Mg}_{0.9}\text{Zr}_{0.1}\text{B}_2$ is much smaller than those around $0.4\text{--}8.0 \mu\text{m}$ in the samples fabricated under high pressure.¹⁷ Besides the reduction of the grain size, very small ZrB_2 particles are formed in the MgB_2 matrix, which has a contribution to flux pinning in Zr-doped samples. At the low doping level of $x=0.05$, the density is higher than pure MgB_2 , but not as high as in $\text{Mg}_{0.9}\text{Zr}_{0.1}\text{B}_2$. Therefore, the J_C value in this sample is larger than that in pure MgB_2 , but much smaller than that in $\text{Mg}_{0.9}\text{Zr}_{0.1}\text{B}_2$. Although the sample with $x=0.2$ has higher density and smaller grain size (30 nm), J_C is still lower than that of $\text{Mg}_{0.9}\text{Zr}_{0.1}\text{B}_2$. This is due to the decrease of the amount of MgB_2 phase and the increase of the ZrB_2 phase.

In summary, highly dense MgB_2 bulk samples can be prepared by Zr doping through solid-state reaction under ambient pressure. The Zr doping leads to the formation of ZrB_2 in the sample and a small substitution of Zr for Mg. By $x=0.1$ doping in $\text{Mg}_{1-x}\text{Zr}_x\text{B}_2$, J_C can be significantly enhanced to $2.1 \times 10^6 \text{ A/cm}^2$ in 0.56 T and $5.7 \times 10^5 \text{ A/cm}^2$ in 2 T at 5 K. At 20 K, J_C is as high as $1.83 \times 10^6 \text{ A/cm}^2$ in self-field, $5.51 \times 10^5 \text{ A/cm}^2$ in 1 T and $1.22 \times 10^5 \text{ A/cm}^2$ in 2 T. Also, this sample has a higher irreversibility field and upper critical field. It can be believed that the excellent grain connection, the reduction of grain size and very small ZrB_2 particles contribute to the great enhancement of the flux pinning.

This work was partially supported by New Energy and Industrial Technology Development (NEDO) of Japan and the Ministry of Science and Technology of China.

- ¹J. Nagamatsu, N. Nakagawa, T. Muranaka, Y. Zenitani, and J. Akimitsu, *Nature (London)* **410**, 63 (2001).
- ²D. C. Larbarlestier, M. O. Rikel, L. D. Cooley, A. A. Polynaskil, J. Y. Jiang, S. Patniak, X. Y. Cai, D. M. Feldman, A. Gurevich, A. A. Squitieri, M. T. Naus, C. B. Eom, E. E. Hellstrom, R. J. Cava, K. A. Regan, N. Rogado, M. A. Hayward, T. He, J. S. Slisky, P. Khalifah, K. Inumara, and M. Haas, *Nature (London)* **410**, 186 (2001).
- ³M. S. Kim, C. U. Jung, M. S. Park, S. Y. Lee, H. P. Kim, W. N. Kang, and S. I. Lee, *Phys. Rev. B* **64**, 012511 (2001).
- ⁴D. K. Finnemore, J. E. Ostenson, S. L. Bud'ko, G. Lapertot, and P. C. Canfield, *Phys. Rev. Lett.* **86**, 2420 (2001).
- ⁵M. Kambara, N. H. Babu, E. S. Sadki, J. R. Cooper, H. Minami, D. A. Cardwell, A. M. Campbell, and I. H. Inoue, *Supercond. Sci. Technol.* **14**, L5 (2001).
- ⁶Y. Takano, H. Takeya, H. Fuji, H. Kumakura, T. Hatano, K. Togano, H. Kito, and H. Ihara, *Appl. Phys. Lett.* **78**, 2914 (2001).
- ⁷H. H. Wen, S. L. Li, Z. W. Zhao, Z. A. Ren, G. C. Che, H. P. Yang, Z. Y. Liu, and Z. X. Zhao, *Chin. Phys. Lett.* **18**, 816 (2001).
- ⁸N. A. Frederick, S. Li, M. B. Maple, V. F. Nesternko, and S. S. Indrakanti, *cond-mat/0106518*.
- ⁹Y. Bugoslavsky, G. K. Perkins, X. Qi, L. F. Cohen, and A. D. Caplin, *Nature (London)* **411**, 561 (2001).
- ¹⁰Y. Feng, J. G. Wen, N. Koshizuka, and L. Zhou, *Appl. Phys. Lett.* **70**, 2984 (1997).
- ¹¹S. M. Kazakov, M. Angst, and J. Karinski, *cond-mat/0103350*.
- ¹²S. Jin, H. Mavoori, and R. B. Vandover, *Nature (London)* **411**, 563 (2001).
- ¹³Y. Zhao, Y. Feng, C. H. Cheng, L. Zhou, Y. Wu, T. Machi, T. Fudamoto, N. Koshizuka, and M. Murakami, *Appl. Phys. Lett.* **79**, 1154 (2001).
- ¹⁴C. P. Bean, *Rev. Mod. Phys.* **36**, 31 (1964).
- ¹⁵J. E. Hirsch, *Phys. Lett. A* **282**, 292 (2001).
- ¹⁶A. M. Campbell and J. E. Evets, *Adv. Phys.* **21**, 199 (1972).
- ¹⁷J. Q. Li, L. Li, Y. Q. Zhou, Z. A. Ren, G. C. Che, and Z. X. Zhao, *Chin. Phys. Lett.* **18**, 680 (2001).